JOURNAL OF MATERIALS SCIENCE 16 (1981) 1980–1988

Conversion of monolithic gels to glasses in a multicomponent silicate glass system

C. J. BRINKER
Sandia National Laboratories, Albuquerque, New Mexico 87185, USA*
S. P. MUKHERJEE
Battelle Columbus Laboratories, Columbus, Ohio 43201, USA

Multicomponent silicate glasses of composition (wt%) $66SiO_2$–$18B_2O_3$–$7Al_2O_3$–$6Na_2O$–$3BaO$ were prepared by three sol–gel processes which differed primarily in the extent of hydrolysis of the metal alkoxide precursors. Gels which were prepared from solutions in which a stoichiometric excess of water was added, causing extensive replacement of OR groups ($R \equiv (C_xH_{(2x+1)})^{-1}$ by hydroxyl groups, were converted to fully dense, organic-free, monolithic glasses at temperatures near the glass transition temperature. Gels containing large numbers of OR groups showed enhanced densification at lower temperatures due to condensation reactions, but these gels could not be converted to fully dense, organic-free glasses. This investigation has shown that at least three possible densification mechanisms might be operative during the gel to glass conversion: volume relaxation, condensation reactions and viscous sintering.

1. Introduction

In the sol–gel process, glass-like macromolecules, containing network-forming cations linked by bridging oxygens, are formed in solution at low temperature by chemical polymerization. The polymerization process normally proceeds, in concentrated solutions, until the solution is transformed to a stiff, amorphous mass referred to as a gel. Recently, Yamane *et al.* [1] reported work on the low temperature conversion of silica gels to monolithic silica glass and Yoldas [2] described conceptually the preparation of monolithic gels for one- and two-oxide systems and their conversion to glasses without melting.

The purpose of this investigation was to prepare multicomponent silica gels of composition (wt%) $66SiO_2$–$18B_2O_3$–Al_2O_3–$6Na_2O$–$3BaO$ and to convert the gels to monolithic glass at low temperatures without melting.

During the gel to glass conversion, both chemical and structural transformations take place which can be summarized as follows [1]: (1) physical desorption of water from micropore walls, (2) pyrolysis of residual organic groups, (3) condensation polymerization, (4) formation and collapse of micropores and (5) viscous sintering. The present study was conducted so that these transformations could be characterized with respect to conversion temperature. When borosilicate glasses of the above composition are prepared by conventional melting of constituent oxides, melting temperatures in excess of 1600° C are employed. The chemical and physical transformations which occur during pyrolysis of a gel generally result in complete conversion of gels to glass at temperatures less than the glass softening point. Therefore, it was expected that dense glass of this composition could be formed by sol–gel processing at a temperature less than 710° C.

In order to investigate the effect of sol–gel processing on the gel to glass conversion, three different sol–gel processes were used to prepare the gels for this study. The three processes differed primarily in the extent of hydrolysis of the metal alkoxide precursors.

The remainder of this paper describes the

*A US Department of Energy Facility.

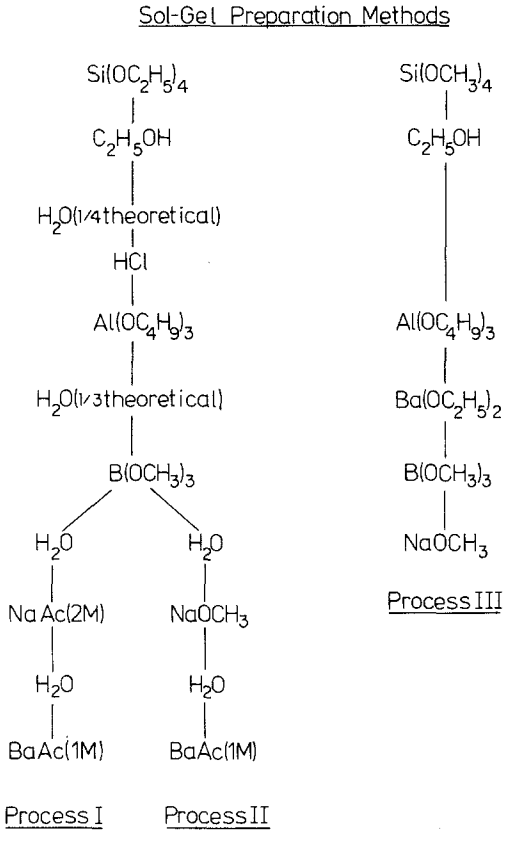

Figure 1 Schematic representation of the three sol–gel processes employed. Theoretical refers to the amounts of water required to result in, for example, one-quarter replacement of OR groups by OH groups.

methods employed to characterize the gel to glass conversion for the three processes employed and shows how, for a particular sol–gel process, dense monolithic glasses were prepared at temperatures only slightly greater than the glass transformation temperature of conventionally melted glass of the investigated composition.

2. Experimental procedure

The three sol–gel processing methods are represented schematically in Fig. 1 and are described in detail elsewhere [3]. Processes I and II were similar to those developed by Thomas [4, 5] and Dislich [6] and reported on by other workers [7–9] in which metal alkoxides of network-forming cations (Si, Al and B) are partially hydrolysed and then polymerized, forming bridging oxygens, as represented in the following reaction sequence:

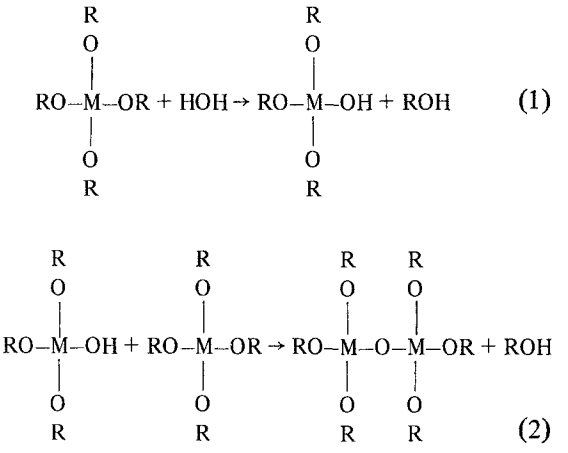

$$RO{-}M(OR)_2{-}OR + HOH \rightarrow RO{-}M(OR)_2{-}OH + ROH \quad (1)$$

$$RO{-}M(OR)_2{-}OH + RO{-}M(OR)_2{-}OR \rightarrow RO{-}M(OR)_2{-}O{-}M(OR)_2{-}OR + ROH \quad (2)$$

where M is Si, Al or B and R is an alkyl group $(C_xH_{(2x+1)})^{-1}$.

In Process I, aqueous solutions of sodium acetate (2M) and barium acetate (1M) were added with additional water, resulting in a total water content 2 to 3 times the stoichiometric amount required to fully hydrolyse the alkoxides. In Process II sodium was added as an alkoxide while barium was added as an aqueous solution of barium acetate (1M). To maintain solution stability, only 90% of the stoichiometric amount of water required to fully hydrolyse the alkoxides could be added to Process II solutions. In Process III all constituents were added as alkoxides in alcoholic solution. Gelation occurred only after exposure of the gels to approximately 80% relative humidity for a period of 2 to 5 days. Due to the minimal amount of water introduced by this process, resultant gels contained high amounts of residual alkyl groups.

Samples were prepared from each process by

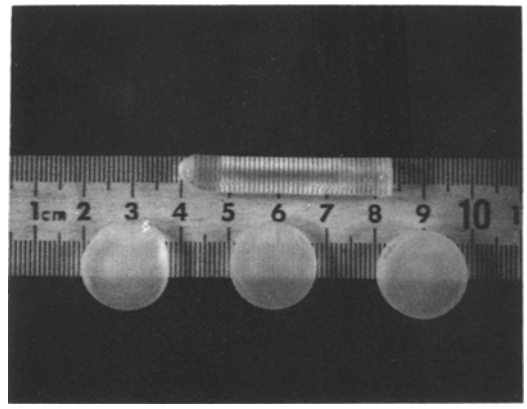

Figure 2 Examples of monolithic cylinders and sliced wafers prepared by slow drying of gels.

casting the solutions in cylindrical Teflon or glass moulds. After gelation the samples were dried slowly at or below 40° C to produce highly porous but optically clear monolithic gels, as shown in Fig. 2. Individual samples were sliced from the cylinders with a diamond saw using no coolant.

The gels were converted to glasses by heat treatment in air at heating rates of $1^\circ C\,min^{-1}$. During the gel to glass conversion, weight loss, due to the removal of organic matter and water from the gels, was measured by thermal gravimetric analysis (TGA). Differential thermal analysis (DTA) and residual gas analysis (RGA, using a quadrupole mass spectrometer) were utilized to interpret the weight loss data. Linear shrinkage was measured using a dual pushrod quartz dilatometer. The shrinkage and weight loss data were combined to follow the densification process.

The changing pore structure of the gels was investigated by direct transmission electron microscopy (TEM) of gel fragments and by analysis of gas adsorption–desorption isotherms [10].

Vickers microhardness was measured as a function of the conversion temperature so that the densification process could be related to changes in physical characteristics.

3. Results and discussion

3.1. Differential thermal analysis

During the conversion of the dried gels to glasses, both residual organic matter and water incorporated during the syntheses were removed by heating to temperatures less than 600° C. Fig. 3 shows comparative DTA curves for equal weights of gels prepared by each process and heated in stagnant air. Gels prepared by all processes showed endothermic behaviour for temperatures between 100 and 200° C, primarily due to removal of physically bound water [11]. Residual organic matter which was removed by combustion processes above 200° C resulted in the exothermic parts of the curves seen in Fig. 3.

In Process I, after initial polymerization of the alkoxides, excess water was added to convert residual organic matter to alcohol as represented in the following reaction

$$M(OR)_x + (\text{excess})\, H_2O \rightarrow M(OH)_x + (x)\, ROH. \quad (3)$$

However, even in excess water, silicon alkoxides do not completely hydrolyse to (OR)-free com-

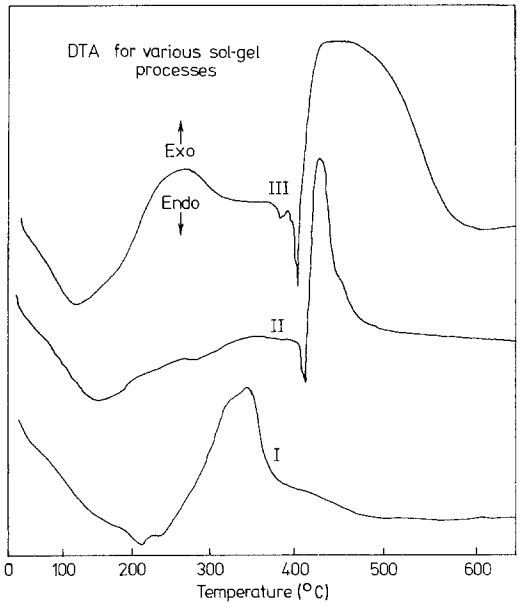

Figure 3 Differential thermal analysis (DTA) traces for equal weights of powdered gels, heated in stagnant air.

plexes [2, 5] so that some residual alkyl groups remained to be combusted at elevated temperatures. Processes II and III incorporated significantly less water in their respective syntheses, less than the stoichiometric amount required to fully hydrolyse the alkoxides. Therefore, more residual organic matter was incorporated in gels produced by Processes II and III. Acetates introduced with the addition of Na and Ba in Processes I and II (Ba only) were not eliminated during the syntheses and therefore were also removed upon heating.

The DTA curve for Process I gels showed two small endothermic peaks slightly above 200° C followed by a broad exothermic peak. RGA of samples heated in both vacuum and air showed that these peaks corresponded primarily to the carbonization and oxidation of acetates.

Process II differed from Process I in that sodium was added as sodium methylate ($NaOCH_3$) and no excess water was used in the synthesis. The DTA curve for Process II gels showed only slight exothermic behaviour between 300 and 400° C attributable to acetate removal. A sharp endothermic peak was observed at 415° C followed by a sharp exothermic peak at 430° C. These two peaks were attributed to removal of alkyl groups associated with metal alkoxides. Similar DTA features were observed for gels of Process III which were prepared totally from alkoxides. In

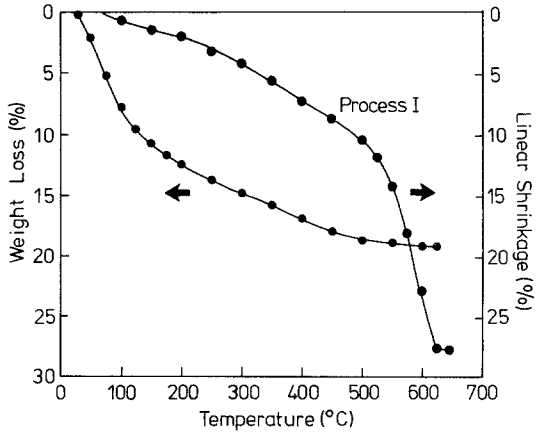

Figure 4 Weight loss and linear shrinkage for Process I gels heated at 1° C min^{-1} in air.

comparison to Process II gels, the distinguishing feature of the DTA curve for Process III gels was the broader exothermic peak which extended from 400 to 575° C. The broadness of this peak implied that the combustion process was limited by the availability of oxygen. Recent work suggests that sharper exothermic peaks can be obtained when the combustion atmosphere is enriched in oxygen [12]. Without oxygen enrichment it was not possible to convert Process II and III gels to organic-free glasses, because the pyrolysis of organic matter was not complete by the temperature at which the continuous pore network began to collapse at a heating rate of 1° C min^{-1}.

3.2. Densification

In conversion of the gels to glass, weight loss and shrinkage occurred simultaneously. Figs 4, 5 and 6

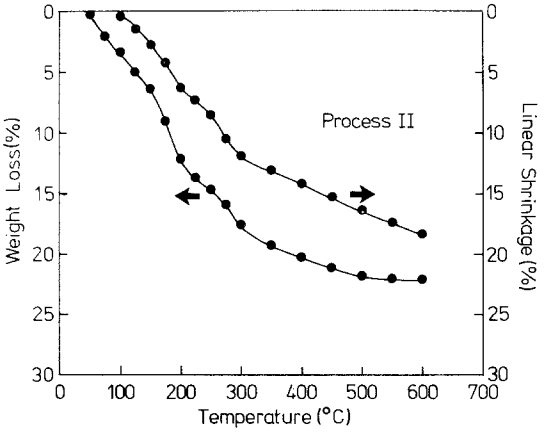

Figure 5 Weight loss and linear shrinkage for Process II gels heated at 1° C min^{-1} in air.

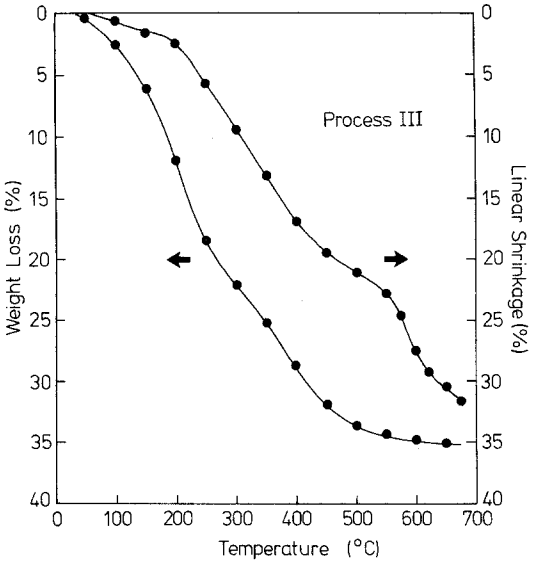

Figure 6 Weight loss and linear shrinkage for Process III gels heated at 1° C min^{-1} in air.

show weight loss and linear shrinkage for gels of Processes I, II and III, respectively, heated at 1° C min^{-1} in stagnant air to 650° C. In Process I, most of the weight loss occurred at temperatures below 150° C and was due primarily to removal of H_2O. Since at these temperatures the gel has an extremely high surface area (400 to 500 m^2 g^{-1}), it was not possible to determine what portion of this weight loss was due to chemically bound rather than physically absorbed water. Above 150° C, higher molecular weight species accounted for most of the weight loss, although water was still evolved, probably as the by-product of condensation reactions of the type

$$-\mathrm{Me}-\mathrm{OH} + \mathrm{HO}-\mathrm{Me}- \rightarrow -\mathrm{Me}-\mathrm{O}-\mathrm{Me}- + \mathrm{H_2O} \quad (4)$$

as suggested by Yamane *et al.* [1] for silica gels.

In heating to 650° C, three regions of differing shrinkage rates were observed for Process I gels. From room temperature, shrinkage occurred at a rather uniform rate (0.02% per °C) to 550° C; however, due to the accompanying weight loss, no net increase in bulk density was observed. If in this temperature range the pyrolysis of organic matter results in micropore formation, a densifying mechanism such as dehydration polymerization (Equation 4) must be operative to maintain the

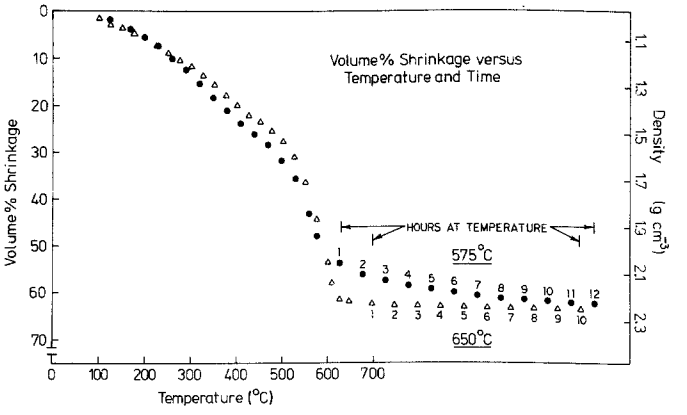

Figure 7 Volume per cent shrinkage and density for Process I gels heated at 1° C min^{-1} and held isothermally at 575 and 650° C. Numbers associated with data points indicate hours of isothermal heat treatments.

initial density. Above 550° C the shrinkage rate increased sevenfold (0.14% per ° C) due to sintering mechanisms driven by the extremely high surface area of the porous network. At 615° C the gel was over 95% dense and the shrinkage rate decreased abruptly. This temperature corresponded to the collapse of the pore structure, as determined by the surface area measurements. When samples were held isothermally at temperatures between 550 and 650° C, fully dense glasses were obtained with time, as shown in Fig. 7.

In comparison to Process I gels, the densification of gels of Processes II and III was quite different. As shown in Figs 5 and 6, weight loss and shrinkage paralleled each other throughout the temperature range so that shrinkage was roughly proportional to weight loss. Because Process II and III gels were less hydrolysed in their syntheses, the resultant gels were likely to be less crosslinked than Process I gels. This has two consequences. First, if less initial crosslinking exists, the gel network should be able to relax to a more compact structure in response to material loss (e.g. alkyl, water, acetates or solvent) during heating. Second, since many residual alkyl groups exist, condensation reactions forming bridging oxygens in place of the large alkyl groups (Equation 2) could occur throughout the heat treatment range. For Process II and III gels, both of these mechanisms should result in enhanced densification at low temperatures as compared to Process I gels, in which significant densification did not occur until T_g (the glass transition temperature), as expected for a more highly crosslinked structure.

Fig. 8 plots density as a function of temperature for a heating rate of 1° C min^{-1}. As shown in this figure, for temperatures up to 550° C, Process II and III gels showed increased densification in comparison to Process I gels. This suggests that,

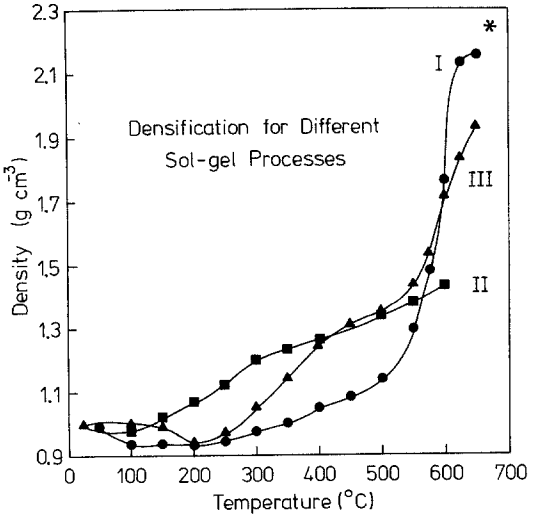

Figure 8 Density against temperature for Process I, (•) II, (▪) and III (▲) gels heated in air at 1° C min^{-1}. Asterisk indicates the density of comparable glasses produced by conventional melting of oxides.

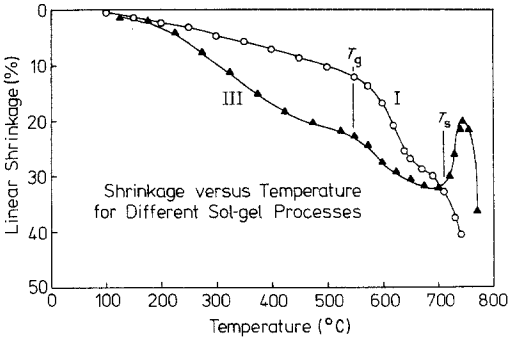

Figure 9 Linear shrinkage against temperature for Process I and III gels. Glass transition (T_g) and softening temperatures (T_s) of conventionally melted glass of this composition are indicated.

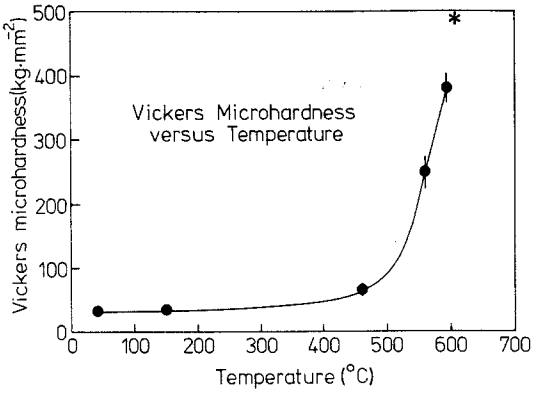

Figure 10 Vickers microhardness against temperature for Process I gels. Asterisk indicates microhardness for conventionally melted glass of this composition.

due to their high reactivity, gels containing large amounts of alkyl groups could perhaps be densified by isothermal heat treatments at temperatures where condensation reaction rates are enhanced.

At a heating rate of $1\,^{\circ}C\,min^{-1}$ only gels of Process I approached full density at temperatures above T_g, where the viscous sintering mechanism took place [13]. Organic matter entrapped within Process II and III gels did not allow them to become fully dense and caused samples to bloat at the glass softening point, as shown in Fig. 9, where comparative linear shrinkages are plotted to 750° C for gels of Processes I and III. At T_g both gels showed enhanced shrinkage due to viscous sintering; however, at the softening point, when the viscosity was greatly reduced, Process I gels flowed, whereas Process III gels bloated, disrupting their monolithic structure.

Vickers microhardness was determined for Process I monoliths as a function of heat treatment temperatures. The similarity of the plot of hardness against temperature (Fig. 10) to that of density against temperature (Fig. 8) suggests that the two parameters are closely related.

3.3. Pore structure

Fig. 11 shows the nitrogen adsorption–desorption isotherm along with a BET plot for a Process I gel heated to 400° C at $1\,^{\circ}C\,min^{-1}$. From analysis of the BET plot, a surface area of $415\,m^2\,g^{-1}$ was obtained. The desorption branch of the isotherm closes almost vertically (at $P/P_s = 0.4$), indicating a very narrow pore size distribution, as shown in Fig. 12 [14].

Fig. 13 shows surface area and Table I lists mode pore opening radius and pore volume all as a function of treatment temperature. The very high values of surface area measured for the gels

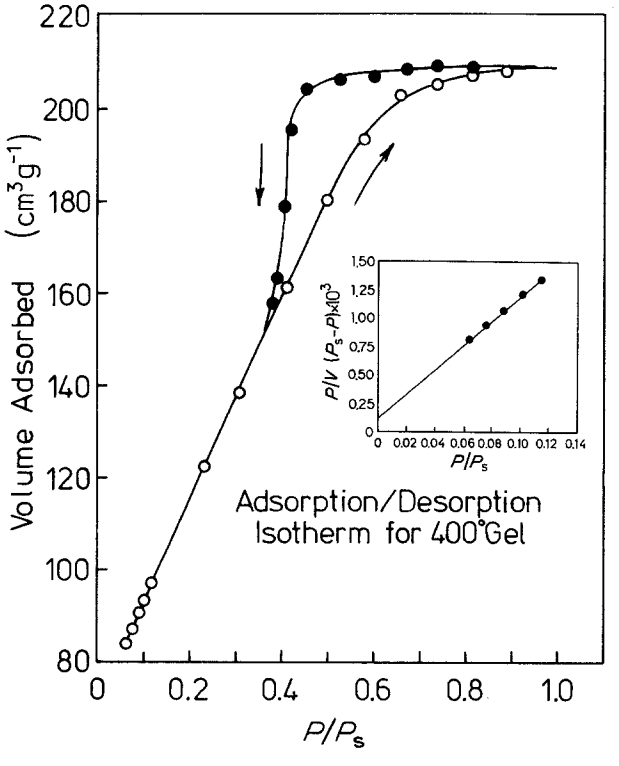

Figure 11 Nitrogen adsorption–desorption isotherm and BET plot (inset) for a 400° C gel prepared by Process I.

TABLE I Pore radius and volume versus heat treatment temperature for Process I gels

(1) Heat treatment (° C)	(2) Mode pore radius (Å)	(3) Pore volume* ($cm^3 g^{-1}$)	(4) Pore volume† ($cm^3 g^{-1}$)	(5) Pore volume‡ ($cm^3 g^{-1}$)
150	15.7	0.23	0.39	0.59
400	16.6	0.20	0.34	0.54
500	17.7	0.16	0.32	0.50

*calculated from desorption isotherms.
†calculated from surface area.
‡calculated from bulk density.

implied that the pore structure remained continuous to temperatures in excess of 500° C. Continuity of the pore structure was also indicated by helium permeability measurements. A helium diffusion coefficient of 10^{-3} cm^2 sec^{-1} at room temperature obtained from the permeability data can only be explained by assuming continuous porosity.

The pore volumes shown in Table I were determined by three different methods. Column 3 contains values calculated from the desorption branches of the respective isotherms [15]. Column 4 contains values calculated from the surface area by assuming the pores to be cylindrical in shape with a uniform cylinder radius equal to the mode pore radius and Column 5 contains values calculated from the bulk density by assuming that the condensed regions of the polymerized gel had the same density as the comparable glass, i.e. 2.27 gm cm^{-3}. The disparity in the results of Columns 3 or 4 with Column 5 indicated that either the gel "polymer" contained a much larger free volume than the comparable glass or that a significant amount of isolated pores existed which did not enter into either surface area or pore volume determinations made from the nitrogen desorption isotherms. Since gels of Process I discoloured when heated to 250° C and, through combustion of organic matter, became colourless again by 400° C, it appeared that all areas of the gel polymer were in close proximity to a continuous porous network; however, the possibility of having additional isolated pores can not be eliminated.

For calculating the pore radii shown in Column 4 it was assumed that pores were of a uniform radius for a particular heat treatment. However, if it is assumed that the pores possessed a corpuscular or necked structure, as suggested by Robinson and Ross [16], lower estimates of pore volume for a particular surface area will result, reducing the discrepancy between Column 3 and 4 values.

If estimates of pore volumes obtained from the nitrogen desorption isotherm are correct (Column 4) and few isolated pores exist, the gel "polymer" density must be considerably lower than that of the comparable glass at temperatures up to 500° C. This would correspond to a higher fictive tempera-

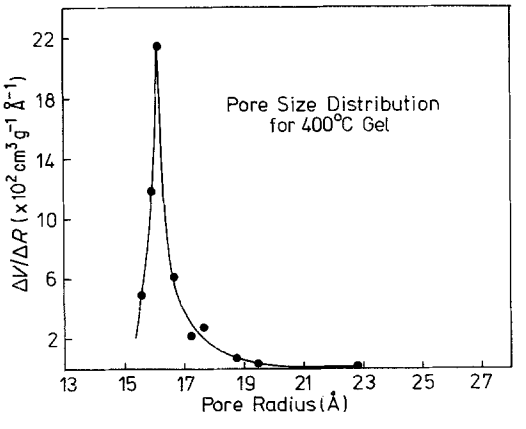

Figure 12 Pore size distribution calculated from the desorption isotherm for a 400° C gel prepared by Process I.

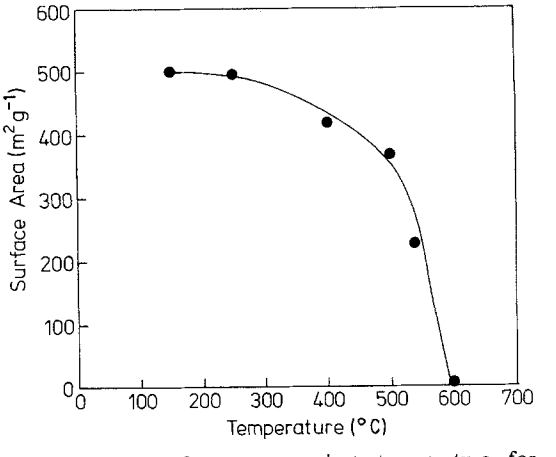

Figure 13 BET surface area against temperature for Process I gels.

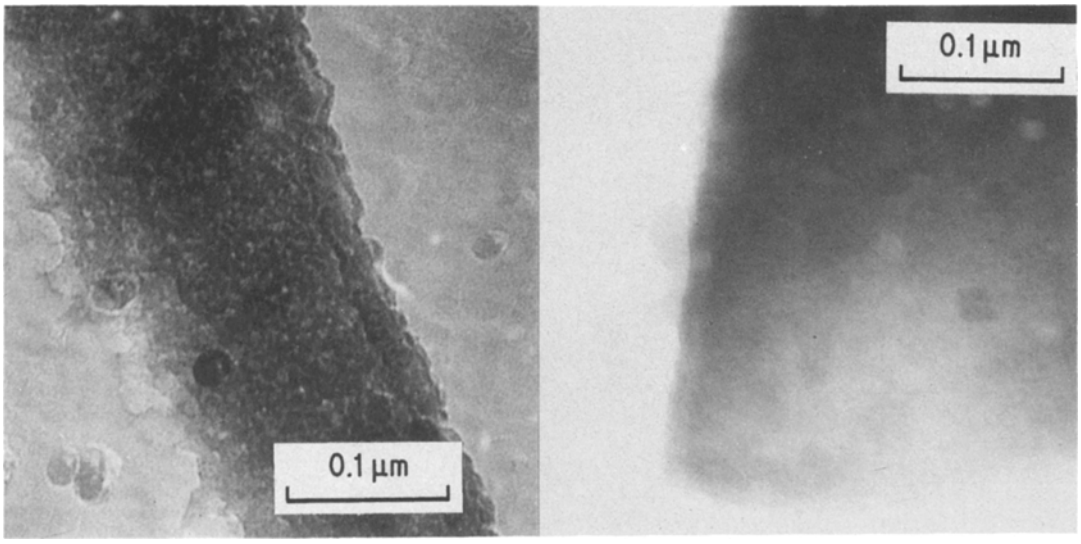

Figure 14 Direct transmission electron micrograph of gel fragments unheated and heated for 12 h at 575° C. Bars indicate 0.1 μm. (Large round features are relics of the underlying carbon film.)

ture, as recently suggested by Puyané *et al.* [17] and shown for silica gels by Yamane *et al.* [1]. At temperatures near the glass transition temperatures, volume relaxation mechanisms would allow the structure to collapse to an equilibrium state, contributing to gel densification.

Transmission electron microscopy was used to substantiate the gas adsorption–desorption data described above. Fig. 14 shows direct transmission micrographs of a Process I gel before and after a 575° C heat treatment for 12 h. From comparison of the unheated gel ($\rho = 1.0\,g\,cm^{-3}$) to the dense 575° C gel ($\rho = 2.25\,g\,cm^{-3}$), it was apparent that the pore structure was interconnected with a narrow size distribution much smaller than 100 Å. However, the superposition of pores made direct pore volume determinations impossible.

4. Conclusions

The various sol–gel processes employed were shown to directly effect the conversion of the resultant gels to monolithic glasses. Gels which were synthesized with excess water (Process I) resulted in polymeric structures which densified at temperatures close to the glass transition temperature of the conventionally melted glass. The densification process was characterized by a rapid decrease in specific surface area along with a rapid increase in microhardness. Condensed regions of the gel were significantly less dense than the comparable glass to temperatures over 500° C. Full densification was achieved by isothermal heat treatments at temperatures less than the glass softening point.

Gels which were synthesized with amounts of water less than the stoichiometric amount required to completely hydrolyse the alkoxides (Processes I and III) showed considerable densification at temperatures less than 500° C due to the removal of alkyl groups by condensation reactions. However, in contrast with Process I, Processes II and III incorporated more residual organic matter into their respective gels. At a heating rate of 1° C min^{-1} or greater this organic matter, primarily alkyl groups, did not completely pyrolyse before the pores began to close. Organic matter was thus entrapped, causing bloating of the glasses and disintegration of their monolithic structure.

This investigation showed that at least three possible densification mechanisms might be operative during the gel to glass conversion: volume relaxation, condensation reactions and conventional sintering. For conversion of monolithic gels to glasses only the sol–gel process, which employed excess water, resulted in optically clear, dense glasses which remained monolithic. Excess water converted most residual organic matter to alcohols and promoted crosslinking of the polymeric structure. Both of these mechanisms appeared important in maintaining the monolithic structure.

Acknowledgements

The authors thank S. M. Lappin for dilatometer measurements, B. M. Schwartz for residual gas analyses and J. E. Shelby for permeability measurements. This work was supported by the US Department of Energy under contract DE-AC04-76-DP00789.

References

1. M. YAMANE, S. ASO, S. OKANO and T. SAKAINO, *J. Mater. Sci.* **14** (1979) 607.
2. B. YOLDAS, *ibid.* **14** (1979) 1843.
3. C. J. BRINKER and S. MUKHERJEE, presented at the 82nd Annual Meeting of the American Ceramic Society, Chicago, IL (1980).
4. I. THOMAS, Patent No. 3 799 754 (1974).
5. *Idem*, Patent No. 4 028 085 (1977).
6. H. DISLICH, *Angew Chemie, Int. Edition* **10** (1971) 363.
7. G. CARTINAN, V. GOTTARDI and M. GRAZIANI, *J. Non-Cryst. Sol.* **29** (1971) 41.
8. K. KAMIJA and S. SAKKA, *Res. Rep. Fac. Eng. Eng., Mie Univ.* **2** (1977) 87.
9. S. P. MUKHERJEE, J. ZARZYCKI and J. P. TRAVERSE, *J. Mater. Sci.* **11** (1976) 341.
10. S. BRUNAUER, P. EMMETT and E. TELLER, *J. Amer. Chem. Soc.* **60** (1938) 309.
11. K. KAMIJA, S. SAKKA and Y. YMANAKA, Proceedings of the 10th International Congress on Glass, Vol. 13 (1974) p. 44.
12. C. R. J. GONZALES OLIVER, P. F. JAMES and H. RAWSON, 12th International Congress on Glass, Albuquerque, New Mexico (1980).
13. M. DECOLTIGNIES, J. PHALIPPOU and J. ZARZYCKI, *J. Mater. Sci.* **13** (1978) 2605.
14. R. VENABLE and W. WADE, *J. Phys. Chem.* **69** (1965) 1395.
15. S. BRUNAUER, R. MIKHAIL and E. BODOR, *J. Colloid Interface Sci.* **24** (1967) 451.
16. E. ROBINSON and R. ROSS, *Canadian J. Chem.* **48** (1970) 2210.
17. R. PUYANÉ, P. JAMES and H. RAWSON, *J. Non-Cryst. Sol.* **41** (1980) 115.

Received 27 October 1980 and accepted 13 January 1981.